Received: July 14, 2019 | Accepted: August 11, 2019 | Web Released: August 22, 2019 CL-190558

Ultra-fast, Selective CO_2 Permeation by Free-standing Siloxane Nanomembranes

Shigenori Fujikawa,*[1,2,3] Miho Ariyoshi,[1,3] Roman Selyanchyn,[1] and Toyoki Kunitake[1,3]
[1]*International Institute for Carbon-Neutral Energy Research (WPI-I2CNER), Kyushu University, 744 Moto-oka, Nishi-ku, Fukuoka 819-0395, Japan*
[2]*Department of Chemistry and Biochemistry, Center for Molecular Systems (CMS), Kyushu University, 744 Moto-oka, Nishi-ku, Fukuoka 819-0395, Japan*
[3]*NanoMembrane Technologies, Inc., 4-1 Kyudai-Shimachi, Nishi-ku, Fukuoka 819-0388, Japan*

E-mail: fujikawa.shigenori.137@m.kyushu-u.ac.jp

Fabrication and gas permselective behavior of free-standing polydimethylsiloxane (PDMS) nanomembranes are discussed. The largest CO_2 permeance is close to 40,000 GPU (the highest one ever reported) at 34-nm membrane thickness without losing the CO_2/N_2 selectivity of 10–12, indicating the formation of pin-hole free nanomembranes.

Keywords: Free-standing nanomembrane | Ultra-fast CO_2 permeation | Direct air capture

The pursuit of efficient CO_2 capture technologies is indispensable and urgently needed to solve the global warming issue. Liquid-scrubbing technology was developed for this purpose and is now operated at the plant scale. However, this process requires large footprints, and the installation sites are limited. On the other hand, CO_2 capture by permselective membranes should be basically advantageous because of its smaller and simpler installations, but this membrane technology is still in its infancy, since the membrane performance, in particular, permeation throughput, is not satisfactory for operating under economically-feasible conditions. Merkel et al. concluded that improved gas permeance is more critical than enhanced selectivity to reduce the cost of CO_2 capture from flue gas in power plants.[1] Many efforts have been devoted to the development of polymeric materials with better CO_2 permeance.[2–5]

Concerning high throughput, membrane thinning is effective for improving the gas permeance of membranes, since the gas flux of the membrane is generally inversely proportional to the membrane thickness. However, straightforward thinning is not necessarily desirable, as the mechanical robustness is lost and pin-hole defects would be readily formed and causes gas leakage.

We reported earlier that large, free-standing nanomembranes were fabricated from organic and inorganic polymers.[6–8] These nanomembranes are characterized by extremely small thickness (down to 20 nm) and macroscopic robustness: the aspect ratio of membrane size and thickness can be greater than one million. The component polymers are various, including epoxy resins, thermosetting resins, and other cross-linking polymers, and the resulting nanomembranes are macroscopically robust and free standing. Such unique features should be useful for the design of novel permselective membranes.

Rubbery poly(dimethylsiloxane) (PDMS) is known to display high gas permeance, due to the highly dynamic nature of the polymer chain as illustrated by low glass transition temperature and large free volume. Frequent uses of PDMS as the gutter layer of multi-layered permselective membranes are based on this physical property.[9–11] It is important to combine the unique material properties of PDMS with the technology of free-standing nanomembranes, for the purpose of exploring high-quality membranes in a practical size. The use of free-standing PDMS membranes was recently reported with respect to mechanical properties and biomaterial applications.[12]

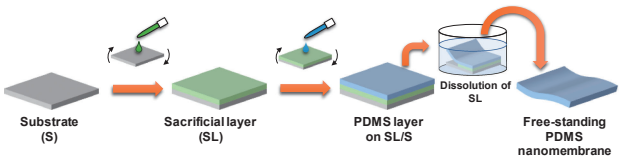

Figure 1. Fabrication of a free-standing nanomembrane.

The preparative procedure for free-standing PDMS nanomembranes is illustrated in Figure 1 and detailed conditions are given in the supporting information. Briefly, a sacrificial layer (SL) of poly(4-hydroxystyrene) (PHS) was spin-coated on a glass substrate, and a PDMS layer was then prepared on the substrate by spin-coating of a Sylgard 184 PDMS solution diluted with hexane. Dissolution of the sacrificial layer in ethanol allowed ready detachment of the PDMS nanomembrane from the substrate. The floating PDMS nanomembranes in ethanol possessed the mechanical strength to maintain their own membrane shape, and they were picked up without breaking from ethanol with a plastic frame or transferred onto a porous support. The thickness of PDMS nanomembranes from ca. 34 to ca. 6700 nm were controlled by changing the spinning speed and the PDMS concentration and confirmed by scanning electron microscopy (SEM) observation. In all cases, the PDMS layers were detached from the substrate without any fragmentation. Figure 2a shows an example of the free-standing films (thickness more than 100 nm) transferred onto O-ring support of 2.5 cm inner diameter. However, maintaining the shapes of the thinner PDMS nanomembranes (thickness of less than 100 nm) was difficult upon picking up in the air. For gas permeation experiments, all the prepared PDMS nanomembranes were successfully transferred onto porous polyacrylonitrile (PAN) support in ethanol. The surfaces of these transferred membranes were very smooth, and no cracks or pinholes were found by SEM observation (maximum resolution of a few nanometers) (Figure 2b). In the cross-sectional observation of Figure 2c, we can clearly see the boundary between the PDMS nanomembrane and the PAN support. The other SEM pictures and membrane thicknesses are summarized in Figure S2 and Table S1.

It must be noted that the precise determination of the permeability-thickness relation was made possible only by transfer fabrication of well-defined PDMS nanomembranes. Thin-film composite (TFCs) approaches have been employed to

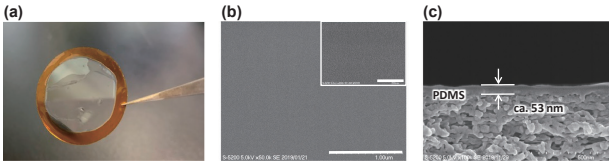

Figure 2. Morphology of a PDMS nanomembrane. (a) Macroscopic appearance of a free-standing and 150-nm thick PDMS nanomembrane (Orange O-ring: a Kapton frame). (b) Surface images of PDMS nanomembrane with the thickness of ca. 53 nm transferred on porous PAN support (scale bar: 1 µm). The inset is the image with higher magnification (scale bar: 200 nm). (c) Cross-sectional image of the PDMS nanomembrane.

avoid the mechanistic weakness of thin permselective membranes.[13] A TFC membrane is usually prepared by a solution-based coating of an ultrathin polymeric selective layer onto a porous support. Unfortunately, the polymer solutions often penetrate into surface pores of the support, and the thickness of the resulting selective layer cannot be well defined. Probably because of this difficulty, the reported CO_2 permeances of PDMS membranes are scattered when the membrane thickness is less than a few hundred nanometers (Table S3). The transfer protocol employed here can give a well-defined interface with the porous supporting layer, as clearly shown in Figure 1c. In contrast, a PDMS nanolayer that is spin-coated directly on a supporting layer gives rise to the irregular interface (Figure S5), probably due to the penetration of the membrane precursor during spin-coating. This irregular interface appears to cause deterioration of the permselective property, as mentioned in the supporting information.

Adhesion via van der Waals interaction should become generally noticeable at the interface of this thickness range. In fact, the 150 nm-thick PDMS layer was not detached from the supporting PAN film even after 10,000 repetitions of film bending (the diameter of bending curvature: 2 mm) shown in Figure S6. This is an additional advantage of using nanometer-thick membranes for multilayer assembly.

The setup of the single gas permeation experiment is schematically shown in Figure S3a. First, membrane permeation of CO_2 and N_2 was investigated separately with pressure differences of 5, 10, 50, 100, 150 and 200 kPa between the feed and permeate sides at the room temperature (25 ± 1 °C). The flux of the permeate gas was monitored by the bubble flow meter. The influence of membrane thickness on gas permeance is summarized in Figure 3. Gas selectivity (CO_2/N_2) for all the membranes remains virtually constant at 10 to 11. This value is close to those of reported PDMS membranes.[14,15] It is noteworthy that all the PDMS membranes at the same thickness showed similar gas permeance and CO_2/N_2 selectivity, irrespective of the pressure change from 10 kPa to 200 kPa. Observation of the invariant selectivity for our nanomembranes is strong proof of the absence of defects and pinholes that would lead to loss of CO_2 selectivity. In our data, membranes of more than one-micrometer thickness display CO_2 permeance in the range of a few thousand GPU and N_2 permeance of less than 300 GPU (1 GPU = 7.5×10^{-12} $m^3(STP)\cdot m^{-2}\cdot s^{-1}\cdot Pa^{-1}$, STP: standard temperature and pressure). These figures essentially agree with the GPU values of about 3800 and 400 for CO_2 and N_2, respectively, with 1-µm-thickness PDMS membranes that were reported for PDMS in the

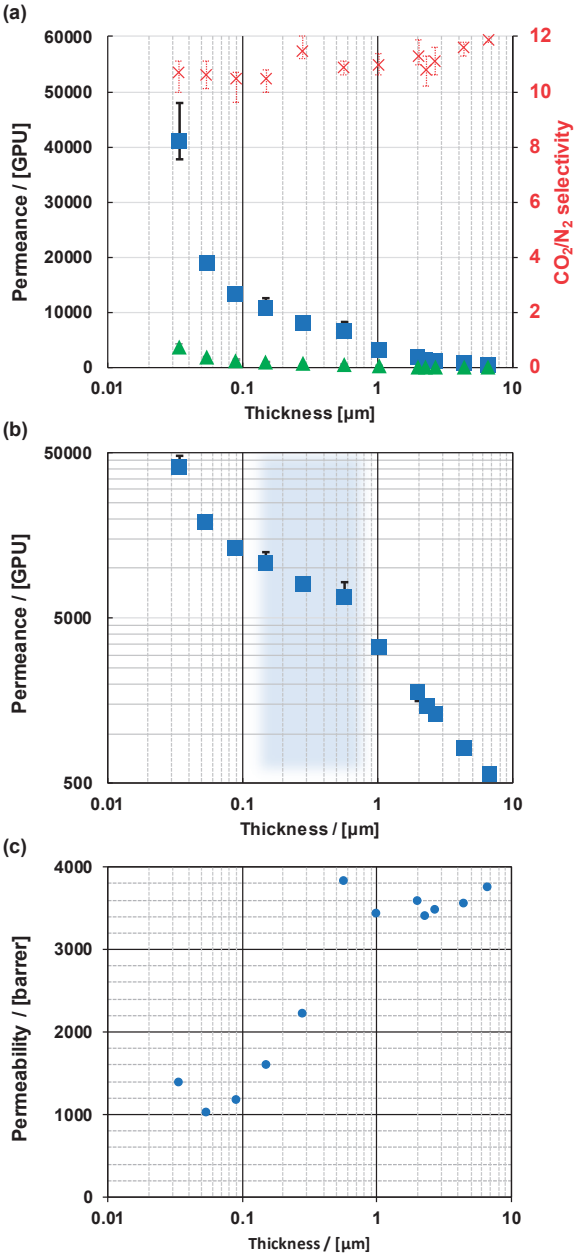

Figure 3. Gas permeance and CO_2/N_2 selectivity of PDMS nanomembranes with different thicknesses. (a) Thickness dependence of CO_2 (blue/square), N_2 (green/triangle) permeances and CO_2/N_2 selectivity (red/cross). (b) Log-log plots of CO_2 permeance and the membrane thickness. Pale blue area corresponds to the transition region. (c) Thickness dependence of CO_2 permeability of PDMS nanomembranes.

commonly used barrer unit by other research groups (1 barrer = 7.5×10^{-2} $m^3\cdot m\cdot m^{-2}\cdot s^{-1}\cdot Pa^{-1}$).[14,16]

A much different situation is found for the thinner PDMS membranes. In the sub-micrometer range, the CO_2 gas permeance is much enhanced, and it exceeds 10,000 GPU at the membrane thickness of less than 100 nm. The CO_2 permeance reaches almost 40,000 GPU at the thickness of 34 nm. This value is much higher than those reported by other groups in the past:

see Table S3. Figure 3b is the log-log plots of the CO_2 permeance data of Figure 3a. Interestingly, the plots appear to be made of two linear relations, and the transition occurs at the thickness of 100 nm to 1 μm. Similar, two-component relations have been found for permselective membranes. Firpo and others mentioned the involvement of the sorption-desorption process in the case of the surface-modified, 200-micrometer-thick PDMS membrane.[17,18] Wijmans et al. and Kattula et al. reported the effect of surface porosity on gas permeance and discussed that such a two-component relationship could arise from different ratios of the pore size of the support layer and the membrane thickness.[19,20]

It has been generally accepted that gas permeability in polymeric materials is inversely proportional to the membrane thickness. This understanding is supported by constant permeability as corrected by thickness. For example, CO_2 permeability of PDMS is about 3800 in the barrer unit that is permeability at 1-micrometer thickness at 35 °C.[14] These results of other workers and us are consistent with the assumption that the permeability is essentially determined by the diffusion process within the polymer matrix. Our permeability results are essentially similar to these previous ones when the membrane thickness is larger than 1 micrometer (Figure 3c and Table S2). However, the CO_2 permeabilities of PDMS nanomembranes decreased with decreasing PDMS thickness as shown in Figure 3c and, thus, such interpretation does not hold for the thinner region, and a different mechanism must be considered. Apparently, the overall rate of the gas permeation is determined by the surface adsorption process and the interior diffusion process for the thin membrane in contrast to only the interior diffusion process for the thick membrane. The gas selectivity may be mostly determined by the surface adsorption process, at least for our case, since it is independent of the membrane thickness.

Our observation of very high CO_2 permeance and reasonable CO_2/N_2 selectivity suggests that the present membrane system should be useful for CO_2 gas capture from dilute emission sources, in spite of the past unsuccessful approaches.[21] In order to confirm this possibility, we conducted the gas permeation experiment at a much lower CO_2 concentration under a small pressure difference by using an experimental setup of Figure S3b. Diluted CO_2 (1000 ppm) in N_2 at atmospheric pressure was used as the feed gas with a very low partial pressure difference of CO_2 across the membrane (as small as 100 Pa). This CO_2 concentration is the lowest limit of detection in our measurement. In this experiment, the flow rate of the feed and sweep gases were set to 100 sccm. The retentate and permeate gases showed similar gas flux (around 100 sccm). The gas concentrations of the retentate and the permeate sides were monitored by gas chromatography, and the results are summarized in Table 1 and Table S4. In the case of a PDMS nanomembrane (thickness: ca. 150 nm), the CO_2 content over the total concentration of CO_2 and N_2 ($[CO_2]/([CO_2] + [N_2])$) at the retentate side was 830 ppm, respectively. On the other hand, a thicker PDMS membrane (thickness: ca. 4400 nm) of the same size gave about 950 ppm. From the comparison of the CO_2 concentration in the retentate side and the feed gas, we can estimate that a PDMS nanomembrane (thickness 150 nm; membrane area 0.785 cm^2) removes about 17% of CO_2, though the thicker membrane captures only 5%. The flux of the sweep and feed gases played an essential role in CO_2 permeation.

Table 1. The CO_2 composition of the feed and retentate gas in the experiments of diluted CO_2 gas separation.

Membrane thickness (μm)	Permeance (GPU)	Feed*,1	Retentate*,1	Removal ratio[2]
4.4	810	996	950	4.6%
0.15	10750	996	832	16.5%

*unit: ppm, [1]the CO_2 content over the total concentration of CO_2 and N_2: $[CO_2]/([CO_2] + [N_2])$, [2]Removal ratio = ([Retentate] − [Feed gas])/[Feed gas] × 100.

Larger flux of the sweep gas gave better CO_2 permeation because the sweep gas removed the permeate CO_2 near the membrane surface, suppressing the concentration polarization of CO_2. It is noteworthy that the amount of the captured CO_2 by the ultrathin PDMS nanomembrane is several times larger than that by the thicker membrane since the CO_2 flux of the thinner nanomembrane (ca. 10750 GPU) is about 13 times higher than that of the thicker counterpart (ca. 810 GPU). The effective concentration of 1000 ppm CO_2 as described here gives hope for the realization of direct air capture by membranes, and further improvement of the present approach could play a decisive role in our efforts against global warming.

In conclusion, we developed well-defined, free-standing PDMS nanomembranes with ultrahigh CO_2 permeance. This defect-free, permselective membrane gave record-high CO_2 permeance close to 40,000 GPU and a CO_2/N_2 selectivity of 10–12 with the PDMS layer of 34 nm thickness. Such high permeability heightens the possibility of CO_2 capture from dilute emission sources like air. In fact, CO_2 extraction from 1000-ppm CO_2 in N_2 was possible. Further elaboration of the membrane property together with proper engineering design will lead to a practical system for direct air capture.

Authors acknowledge Prof. Atsushi Shishido and Prof. Norihisa Akamatsu for their kind support in the film bending measurement. This work was supported by the World Premier International Research Center Initiative (WPI), MEXT, Japan. We gratefully acknowledge the financial support from a Grant-in-Aid for Scientific Research on Innovative Area "Coordination Asymmetry" (No. 16H06513).

Supporting Information is available on https://doi.org/10.1246/cl.190558.

References

1 T. C. Merkel, H. Lin, X. Wei, R. Baker, *J. Membr. Sci.* **2010**, *359*, 126.
2 P. M. Budd, E. S. Elabas, B. S. Ghanem, S. Makhseed, N. B. McKeown, K. J. Msayib, C. E. Tattershall, D. Wang, *Adv. Mater.* **2004**, *16*, 456.
3 P. M. Budd, K. J. Msayib, C. E. Tattershall, B. S. Ghanem, K. J. Reynolds, N. B. McKeown, D. Fritsch, *J. Membr. Sci.* **2005**, *251*, 263.
4 P. M. Budd, N. B. Mckeown, B. S. Ghanem, K. J. Msayib, D. Frutsch, L. Starannikova, N. Belov, O. Sanfirova, Y. Yampolskii, V. Shantarovich, *J. Membr. Sci.* **2008**, *325*, 851.
5 C. H. Lau, P. T. Nguyen, M. R. Hill, A. W. Thornton, K. Konstas, C. M. Doherty, R. J. Mulder, L. Bourgeois, A. C. Y.

Liu, D. J. Sprouster, J. P. Sullivan, T. J. Bastow, A. J. Hill, D. L. Gin, R. D. Noble, *Angew. Chem., Int. Ed.* **2014**, *53*, 5322.
6 M. Hashizume, T. Kunitake, *Langmuir* **2003**, *19*, 10172.
7 R. Vendamme, S. Onoue, A. Nakao, T. Kunitake, *Nat. Mater.* **2006**, *5*, 494.
8 H. Watanabe, R. Vendamme, T. Kunitake, *Bull. Chem. Soc. Jpn.* **2007**, *80*, 433.
9 K. A. Lundy, I. Cabasso, *Ind. Eng. Chem. Res.* **1989**, *28*, 742.
10 R. W. Baker, B. T. Low, *Macromolecules* **2014**, *47*, 6999.
11 W. Yave, A. Car, J. Wind, K.-V. Peinemann, *Nanotechnology* **2010**, *21*, 395301.
12 E. Kang, J. Ryoo, G. S. Jeong, Y. Y. Choi, S. M. Jeong, J. Ju, S. Chung, S. Takayama, S.-H. Lee, *Adv. Mater.* **2013**, *25*, 2167.
13 P. Li, Z. Wang, W. Li, Y. Liu, J. Wang, S. Wang, *ACS Appl. Mater. Interfaces* **2015**, *7*, 15481.
14 T. C. Merkel, V. I. Bondar, K. Nagai, B. D. Freeman, I. Pinnau, *J. Polym. Sci., Part B: Polym. Phys.* **2000**, *38*, 415.
15 P. Li, H. Z. Chen, T.-S. Chung, *J. Membr. Sci.* **2013**, *434*, 18.
16 S. M. Allen, M. Fujii, V. Stannett, H. B. Hopfenberg, J. L. Williams, *J. Membr. Sci.* **1977**, *2*, 153.
17 G. Firpo, E. Angeli, L. Repetto, U. Valbusa, *J. Membr. Sci.* **2015**, *481*, 1.
18 G. Firpo, E. Angeli, P. Guida, R. L. Savio, L. Repetto, U. Valbusa, *Sci. Rep.* **2018**, *8*, 6345.
19 J. G. Wijmans, P. Hao, *J. Membr. Sci.* **2015**, *494*, 78.
20 M. Kattula, K. Ponnuru, L. Zhu, W. Jia, H. Lin, E. P. Furlani, *Sci. Rep.* **2015**, *5*, 15016.
21 E. S. Sanz-Pérez, C. R. Murdock, S. A. Didas, C. W. Jones, *Chem. Rev.* **2016**, *116*, 11840.